Diffusely Infiltrating Gliomas With Poor Prognosis, *TERT* Promotor Mutations, and Histological Anaplastic Pleomorphic Xanthoastrocytoma-Like Appearance Classify as Mesenchymal Type of Glioblastoma, IDH-wildtype by Methylation Analysis

Yoshihiro Tsukamoto, MD, PhD *, **Manabu Natsumeda, MD, PhD***, **Haruhiko Takahashi, MD*‡**, **Jotaro On, MD*‡**, **Hiroki Seto, MD***, **Taiki Saito, MD***, **Kohei Shibuya, MD***, **Ryosuke Ogura, MD, PhD***, **Junko Ito, MD, PhD‡**, **Masayasu Okada, MD, PhD***, **Makoto Oishi, MD, PhD***, **Hiroshi Shimizu, MD, PhD‡**, **Kouichirou Okamoto, MD, PhD§**, **Akiyoshi Kakita, MD, PhD‡**, **Yukihiko Fujii, MD, PhD***

*Department of Neurosurgery, Brain Research Institute, Niigata University, Niigata, Japan; ‡Department of Pathology, Brain Research Institute, Niigata University, Niigata, Japan; §Department of Translational Research, Brain Research Institute, Niigata University, Niigata, Japan

Correspondence: Yoshihiro Tsukamoto, MD, PhD, Department of Neurosurgery, Brain Research Institute, Niigata University, 1-757 Asahimachi-dori, Chuo-ku, Niigata-shi, Niigata-ken, 951-8585, Japan. Email: yoshi.tsukamoto@me.com

Received, October 18, 2022; **Accepted,** February 23, 2023; **Published Online,** May 19, 2023.

BACKGROUND: Pleomorphic xanthoastrocytoma (PXA) (World Health Organization grade II) is classified as a relatively benign and circumscribed glioma; however, anaplastic PXA (APXA, World Health Organization grade III) has a poorer prognosis, and differentiating from glioblastoma can be difficult both histologically and molecularly.

OBJECTIVE: To describe the clinical, pathological, and molecular characteristics of diffusely infiltrating gliomas with histological APXA-like features.

METHODS: Four diffusely infiltrating gliomas in adult patients histologically diagnosed as APXAs at a single institute were retrospectively reviewed. We analyzed their clinical, radiological, pathological, genetic, epigenetic, and prognostic characteristics.

RESULTS: All tumors histologically showed classical characteristic PXA-like appearance with *BRAF* wildtype, mitotic figure, necrosis, and an increased mindbomb E3 ubiquitin-protein ligase 1 labeling index and were initially diagnosed as APXAs; moreover, they underwent high-grade glioma treatment. Three patients with *TERT* promotor mutations died within 18 months. These patients' MRIs showed widespread infiltrating fluid-attenuated inversion recovery hyperintense lesions and Gd-enhancing lesions in the bilateral cerebral hemispheres in 2 of the patients. Contrastingly, a patient with the wildtype *TERT* promotor has survived for 2.5 years without recurrence. MRI revealed an unilateral fluid-attenuated inversion recovery hyperintense and Gd-enhancing lesion. By methylation classifier analysis, all 4 cases clustered toward GBM, IDH-wildtype, mesenchymal type, although one was deemed unclassifiable due to a low calibrated score.

CONCLUSION: In diffusely infiltrating gliomas showing histological characteristics of APXA, methylation classification should be performed as these tumors may be difficult to differentiate between glioblastoma, IDH-wildtype by histological or genetic analysis. The aggressive nature of these tumors should be expected, especially in cases that are *BRAF*-wildtype and *TERT* promotor mutant.

KEY WORDS: Glioblastoma, Anaplastic pleomorphic xanthoastrocytoma, *TERT* promotor, MRI, *CDKN2A/2B*

Neurosurgery Practice 2023;4(2):e00040. https://doi.org/10.1227/neuprac.0000000000000040

Pleomorphic xanthoastrocytoma (PXA) is a rare circumscribed primary central nervous system (CNS) tumor that accounts for <1% of all astrocytomas and has a relatively favorable clinical course. In 1972, Kepes et al[1] defined PXA as a grade II CNS tumor based on the World Health Organization (WHO) classification in 1993. PXA commonly affects children

ABBREVIATIONS: APXA, anaplastic pleomorphic xanthoastrocytoma; **BEV,** bevacizumab; **CNS,** central nervous system; **Gd,** gadolinium; **GFAP,** glial fibrillary acidic protein; **IDH,** isocitrate dehyodrogenase; **INI1,** integrase interiactor 1; **KPS,** Karnofsky performance status; **LI,** labeling index; **MIB1,** mindbomb E3 ubiquitin-protein ligase 1; **OS,** overall survival; **PXA,** pleomorphic xanthoastrocytoma; **SRT,** stereotactic radiotherapy; ***TERT,*** telomerase reversed transcriptase; **TMZ,** temozolomide.

Supplemental digital content is available for this article at neurosurgerypractice-online.com.

and young adults, with a median age at diagnosis approximately 20 years.[2-4] For PXA with mitotic activity <5 mitosis per 10 high-power fields, the 5-year progression-free survival (PFS) and overall survival (OS) rates are 70.9% and 90.4%, respectively.[5]

Patients with PXA may present an aggressive clinical course characterized by mitotic rates ≥5 per 10 high-power fields with or without necrosis, which was defined as "anaplastic PXA" (APXA) (WHO grade III) in the WHO 2016 update. APXAs account for 10% to 22% of all PXA and have worse prognosis than grade II PXA.[5-9] The PFS and OS of primary APXA are 20 and 87 months, respectively, while the corresponding 5-year PFS and OS rates are 48.9% and 57.1%.[5] Because the differential diagnosis between APXA and GBM can be very difficult by histological and genetic analysis, a comprehensive molecular diagnosis using the methylation classification is recommended.[10-12] Given the rarity of APXA, the prognosis, related gene alterations, and optimal treatment protocol remain unclear.[13]

Accordingly, we aimed to describe 4 cases of middle-aged and older patients whose brain tumors were histologically diagnosed as APXA and treated using a high-grade astrocytic tumor regimen. Three patients had aggressive clinical courses and died within 18 months. The 3 patients with poorer prognosis had tumors harboring *TERT* promotor mutations as well as diffusely infiltrating lesions of bilateral hemispheres on MRI. Methylation classifier analysis showed that all 4 cases clustered toward glioblastoma, IDH-wildtype, mesenchymal type, although one was not definitive due to a low calibration score. These molecular and MRI findings could be correlated with worse prognosis and navigate the diagnosis toward glioblastoma, mesenchymal type rather than APXA.

METHODS

Patient Population

Four consecutive adult patients treated at our single institute between April 2010 and March 2021 were histopathologically diagnosed as primary APXA by 2 experienced neuropathologists (H.S. and A.K.) with consensus; accordingly, they underwent surgical removal, and adjuvant therapy for high-grade astrocytoma was administered. Preoperative MRI scans, including pre–Gd-enhanced and post–Gd-enhanced T1-weighted and fluid-attenuated inversion recovery (FLAIR) images, were available for all patients. This study was approved by the Institutional Review Board of Niigata University (Approval No. 2019-0185 and G2022-0012), and patient consent was waived due to the retrospective nature of this study. Case 1 had been included in a previous report on 19 patients with PXA.[8]

Histology and Immunohistochemistry

Surgical specimens were fixed in 10% buffered formalin and embedded in paraffin. Histopathological examination was performed using 4-μm thick sections as previously described.[14] We used primary monoclonal antibodies against the following antigens (**Supplemental Digital Content 1**, http://links.lww.com/NEUOPEN/A60). Immunohistochemical analysis was independently evaluated by Y.T., H.S., and A.K. The mindbomb E3 ubiquitin-protein ligase 1 labeling index (MIB1 LI) was determined using Gunma-LI, a plug-in of Image J.[15] Pathological diagnosis was performed according to WHO Classification of Tumors of the CNS Revised Fourth Edition (2016).

DNA Extraction, PCR, and Direct Sequence

Genomic DNA was extracted from paraffin-embedded sections or frozen tissue as previously described.[16] The primer sequences are shown in **Supplemental Digital Content 2**, http://links.lww.com/NEUOPEN/A61. Subsequently, the PCR products were sequenced on a 3130xl Genetic Analyzer (Applied Biosystems, Foster City, CA, USA) with a Big Dye Terminator v1.1 Cycle Sequencing Kit (Applied Biosystems) following the manufacturer's instructions.[17]

Multiplex Ligation-dependent Probe Amplification

Copy number analyses of *CDKN2A/2B* and mutant *IDH1/2* were conducted through multiplex ligation-dependent probe amplification. The probe mix P088-C2 was used following the manufacturer's instructions (SALSA multiplex ligation-dependent probe amplification KIT; MRC-Holland).[17] Data were analyzed using Coffalyzer.Net Software (MRC-Holland). The thresholds for copy number detection were chosen as previously described and set at 0.8 to 1.2. A ratio of 0.4 was set as the threshold between heterozygous and homozygous losses; in addition, ratios >2.0 were defined as amplifications.[18-20]

DNA Methylation Classification Profiling

The Infinium Methylation EPIC (850 k) BeadChip array (Illumina) was used according to the manufacturer's instructions. Brain tumor classifier version v12.5 was applied for classification of tumors with the free web platform system supplied by the German Cancer Research Center (DKFZ) (https://www.molecularneuropathology.org).[10,21] A calibration score of 0.9 or higher was considered as classifiable.

RESULTS

Clinical and Imaging Characteristics

The 4 patients were 3 men and 1 woman (age 52-84 years, mean 69.8 years). One patient presented with behavior disorder, 2 patients with cognitive dysfunction, and 1 patient with headache, respectively (Table 1). All patients showed FLAIR hyperintense and Gd-enhancing lesions with cystic or non–Gd-enhancing areas. Three patients showed FLAIR hyperintense lesions in the bilateral cerebral hemispheres. Case 1 (Figure 1A) and Case 2 (Figure 1B) showed Gd-enhancing lesions in the bilateral cerebral hemispheres as well as bilateral diffusely infiltrating lesions. Case 3 (Figure 1C) had bilateral thalamic FLAIR hyperintense lesions, with a Gd-enhancing lesion in the right temporal lobe. Case 4 (Figure 1D) had a Gd-enhancing lesion and a surrounding FLAIR hyperintense lesion in the unilateral cerebral hemisphere. Clinical features are presented in Table 1.

Surgical and Postsurgical Treatments

All patients underwent maximum safe resection of Gd-enhancing lesions. Two patients with a unilateral Gd-enhancing lesion received total resections, while partial removal of bilateral Gd-enhancing

TABLE 1. Summary of the Characteristic of 4 Patients

Case	Age	Sex	Symptom	CE lesion	FLAIR lesion	Cyst	Nodule	Extent of resection	Adjuvant therapy	Maintenance therapy	Preoperative KPS	Postoperative KPS	PFS	Therapy at recurrence	OS (follow-up)	Outcome
1	74	M	Behavior disorder	Bil. F	Bil. F	+	+	PR (Lt.)	60 Gy/30 fr + TMZ	TMZ	70	90	4M	SRT (40 Gy/ 8 fr)	9M	Dead
2	84	M	Cognitive decline	Bil. F	Bil. F, Rt. T	+	+	PR (Lt.)	39 Gy/13 fr	TMZ	80	90	4M	TMZ + BEV	9M	Dead
3	52	F	Cognitive decline	Rt. T	Bil. thalamus	+	+	CE lesion STR	60 Gy/30 fr + TMZ	TMZ	50	90	15M	TMZ + BEV + SRT (30 Gy/10 fr)	18M	Dead
4	69	M	Headache	Rt. T	Rt. F, T,	+	+	CE lesion STR	60 Gy/30 fr + TMZ	TMZ	70	80	N/A	N/A	2.5Y	Alive

BEV, bevacizumab; GdCE, gadolinium contrast-enhancing lesion; KPS, Karnofsky performance status, OS, overall survival; PFS, progression-free survival; PR, partial resection; STR, subtotal resection; SRT, stereotactic radiotherapy; TMZ, temozolomide.

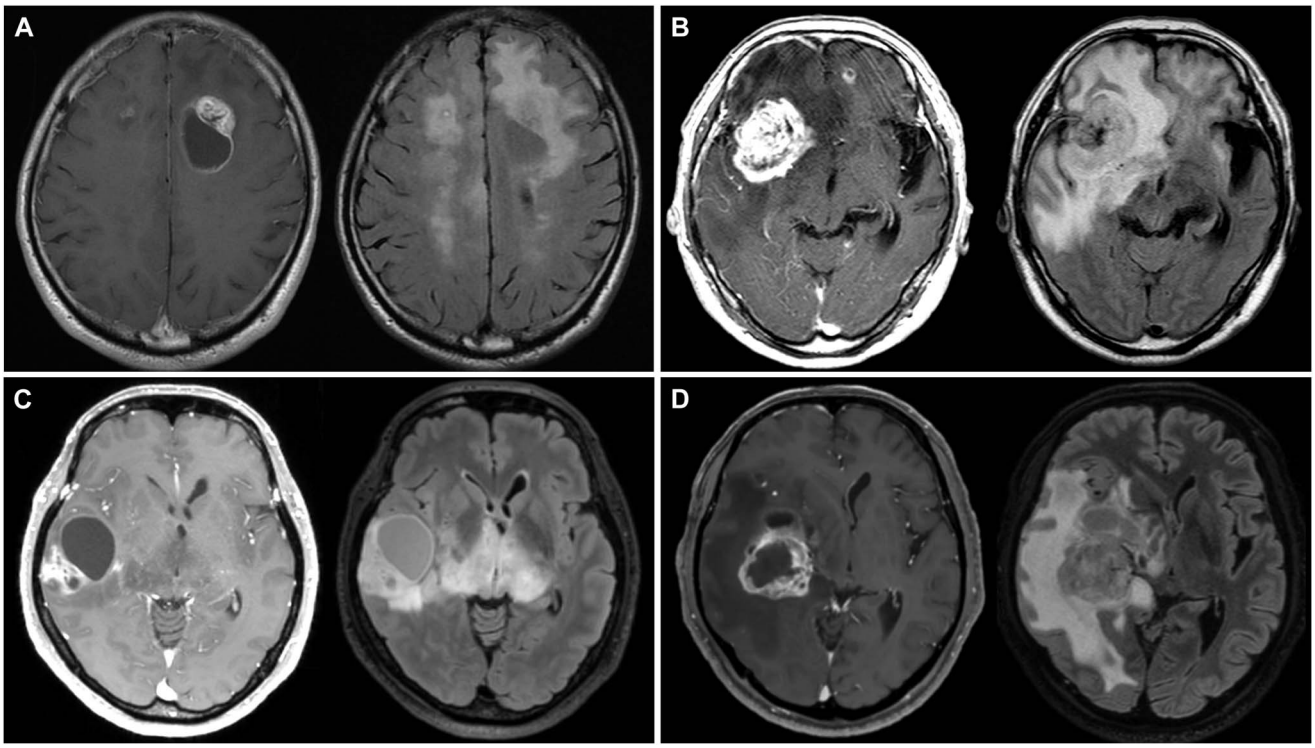

FIGURE 1. *Head MRI findings. The right panel shows the axial gadolinium-enhanced T1WI, and the left panel shows the axial FLAIR image.* **A**, *and* **B**, *Cases 1 and 2 show bilateral diffusely infiltrating FLAIR hyperintense lesions and gadolinium-enhancing lesions in both cerebral hemispheres.* **C**, *Case 3 shows bilateral thalamic FLAIR hyperintense lesions and a unilateral gadolinium-enhancing lesion.* **D**, *Case 4 shows a unilateral gadolinium-enhancing lesion and a surrounding FLAIR hyperintense lesion.*

lesions was achieved in the other 2 patients (**Supplemental Digital Content 3** and **4**, http://links.lww.com/NEUOPEN/A62 and http://links.lww.com/NEUOPEN/A63). Three patients younger than 75 years underwent local irradiation (60 Gy/30 fractions (fr)) in combination with temozolomide (TMZ). Hypofractionated local irradiation (39 Gy/13 fr) was performed on an 84-year-old older patient (**Supplemental Digital Content 3** and **4**, http://links.lww.com/NEUOPEN/A62 and http://links.lww.com/NEUOPEN/A63). All the patients received adjuvant TMZ.

Postsurgical Courses and Outcomes

A therapeutic effect was observed in all patients with decreased FLAIR hyperintense lesions. However, 3 patients with bilateral FLAIR hyperintense lesions showed recurrence. Earlier recurrence and shorter survival were observed in 2 patients with advanced ages and bilateral infiltrating FLAIR hyperintense and Gd-enhancing lesions in both cerebral hemispheres. Case 1 relapsed after 4 months; stereotactic radiotherapy (SRT; 40 Gy/8 fr) was performed; however, the patient died at 9 months after surgery. Case 2 relapsed after 4 months; subsequently, he received combined chemotherapy with bevacizumab (BEV) and TMZ; however, the patient succumbed to disease progression after 9 months. MRI in cases 1 and 2 did not show any therapeutic effects after recurrence. In Case 3, there was a dramatic decrease in bilateral thalamic FLAIR hyperintense lesions 1 year after treatment. However, MRI at 15 posttreatment months showed recurrence in the cerebellum with ataxia. Subsequently, she underwent chemotherapy combined with TMZ, BEV, and SRT (30 Gy/10 fr); however, she died after 18 months of treatment. Case 4 had a unilateral Gd-enhancing lesion with a surrounding FLAIR hyperintense area; moreover, the patient survived for >2.5 years without recurrence after surgery with radiotherapy and 12 treatment courses with TMZ. The 1-year and 2-year survival rates were 50% and 25%, respectively (**Supplemental Digital Content 5**, http://links.lww.com/NEUOPEN/A64). The mean postrecurrence survival period of 3 patients was 4.3 month (range: 3-5 months).

Results from Pathological, Immunohistochemical, Genetic, and Methylation Classifier Examinations

In addition to characteristic PXA features of pleomorphism, presence of xanthomatous cells and eosinophilic granular bodies, and both glial and neuronal differentiation, all tumors showed mitosis and necrosis. Microvascular proliferation and a sarcomatous component were observed in Case 2 (Figure 2A-D, Table 2). INI1 was retained in the sarcomatous component as well as other PXA components (data not shown). Gitter staining revealed abundant reticulin fibers surrounding individual tumor cells. The

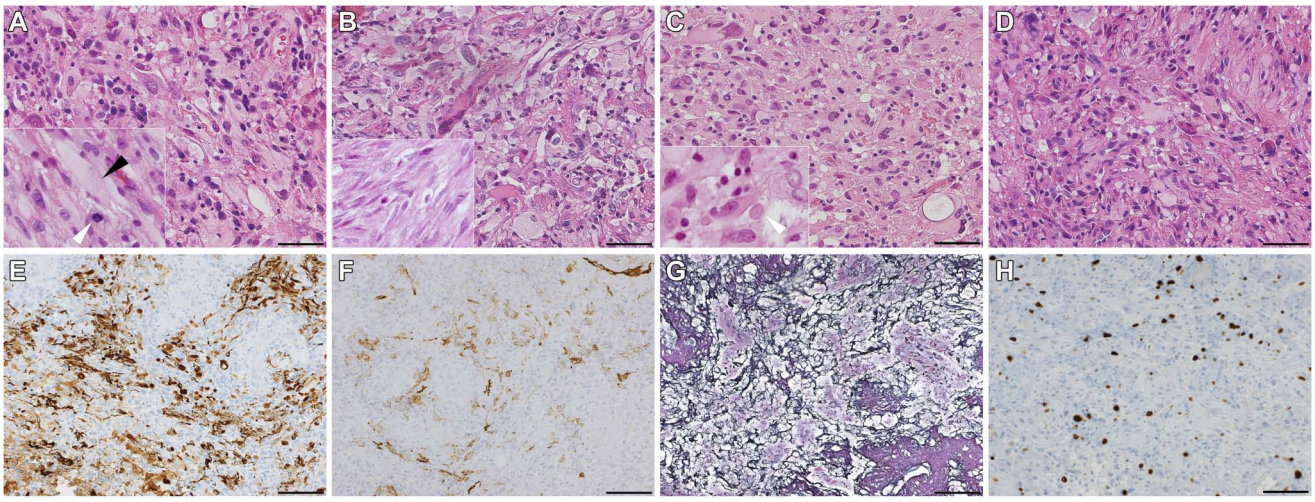

FIGURE 2. *Pathological findings (40×, bar = 100 μm).* **A-D***: H & E staining. Xanthomatous cells and eosinophilic granular bodies are shown in the specimens obtained from* **A***, Case 1,* **B***, Case 2,* **C***, Case 3, and* **D***, Case 4. Especially, the inserted image at the left inferior corner in a white square shows a typical xanthomatous cell, mitosis,* **A***, and eosinophilic granular bodies* **C***, respectively.* **B***, Sarcomatous components observed in Case 2 are shown in the inserted image.* **E-H***, Immunohistochemical staining of Case 1 as a representative case.* **E***, GFAP expression is observed in pleomorphic cells,* **F***, with partially positive CD34 expression.* **G***, Gitter staining shows reticulin fibers;* **H***, moreover, the MIB1 labeling index is approximately 12.8%.*

MIB1 LI increased from 12.8% to 39.5%. Immunohistochemistry examination revealed GFAP, nestin, synaptophysin, and CD34 positivity in all cases. Except for Case 4, neurofilament protein was positive in the other 3 cases. These findings suggested polymorphic differentiation. O6-methylguanine DNA methyltransferase (MGMT) was positive in all cases (Table 2). GFAP, CD34, gitter, and MIB1 immunohistochemistry of Case 1 are presented (Figure 2E-H).

Genetic analysis revealed wildtype *BRAF* V600E, wildtype *IDH1/2*, and wildtype histone H3; moreover, p53 immunohistochemistry was strongly positive in all cases. Heterozygous *CDKN2A2/B* deletion was detected in 2 cases. *TERT* promotor mutations (C228T) were found in 3 patients. The remaining patient lacked both *TERT* promotor mutations and *CDKN2A/2B* deletion (Figure 3).

In addition, methylation classifier was performed. Cases 2, 3, and 4 were classified as glioblastoma, IDH-wildtype, and mesenchymal type with a high calibrated score of >0.9. Case 1 was also considered to be glioblastoma, IDH-wildtype, and mesenchymal type but was not classified due to a low calibration score of 0.87849 (Table 3).

DISCUSSION

We included 4 patients (aged 52-84 years) who were histologically diagnosed primary APXA. The 3 patients with *TERT* promotor mutations with bilateral FLAIR hyperintense lesions showed poorer prognosis (survival ≤18 months) than previously reported patients with primary APXA.[22] All 4 cases were classified as glioblastoma, IDH-wildtype, and mesenchymal type by methylation classifier analysis, although one case had a low calibration score.

As reported by Kepes et al[1] in 1979, PXA originates from subpial astrocytes. PXA cells express neuronal and glial markers.[9,23,24]

TABLE 2. Summary of the Histological Characteristics of 4 Patients

Case	Age	M/F	Pleomorphism	Mitosis	MVP	Necrosis	MGMT	MIB1 LI (%)	GFAP	Nestin	Synaptophysin	NFP	CD34	Sarcomatous component
1	74	M	+	+	+	+	+	12.8%	+	+	+	+	±	–
2	84	M	+	+	+	+	±	30.0%	+	+	+	±	+	+
3	52	F	+	+	+	Micronecrosis	+	24.9%	+	+	+	+	+	–
4	69	M	+	++	+	+	+	39.5%	+	+	±	–	+	–

CD, cluster difference; GFAP, glial fibrillary acidic protein; MGMT, O6-methylguanine DNA methyltransferase; MVP, microvascular proliferation; NFP, neurofilament protein.

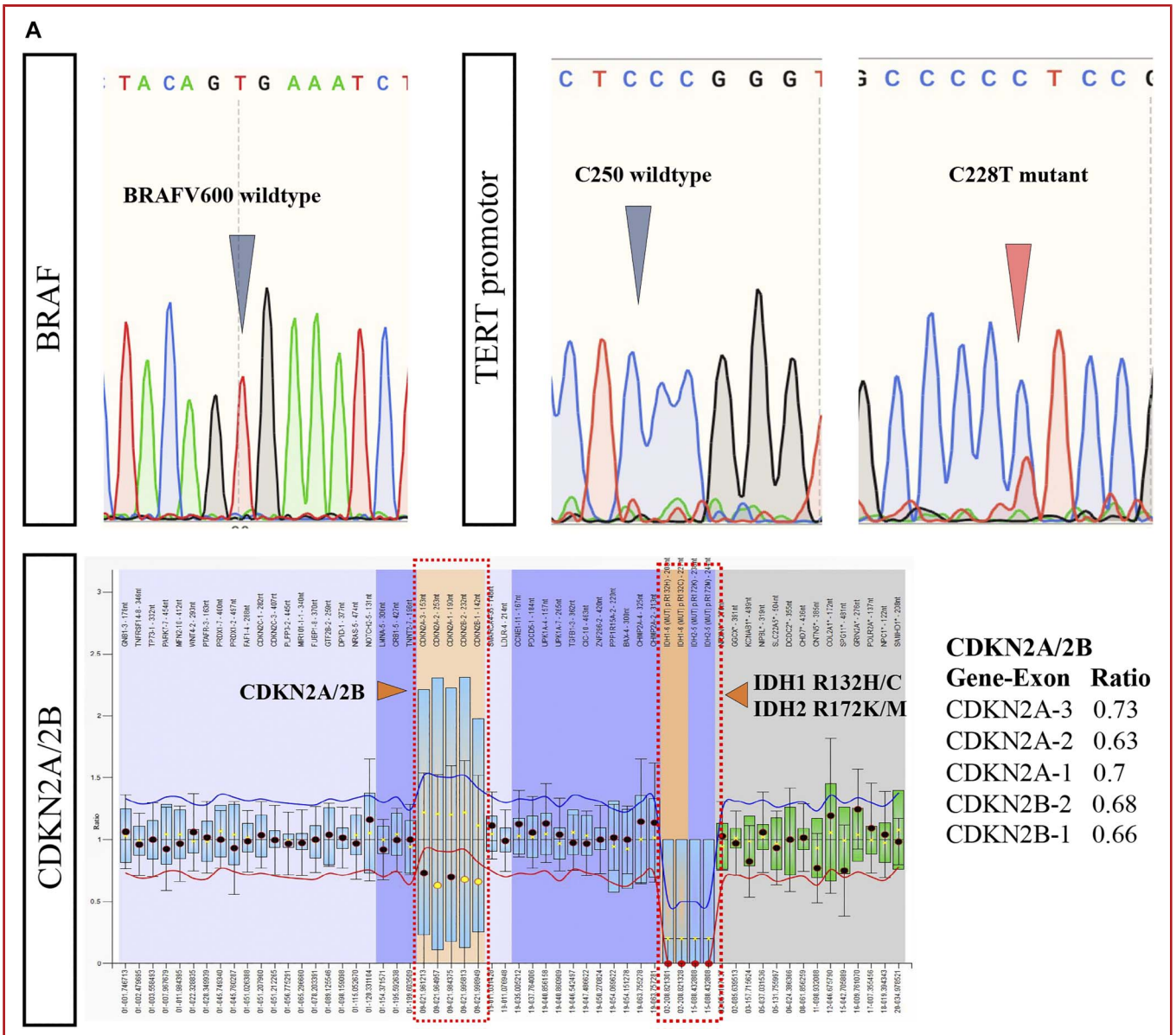

FIGURE 3. *Molecular findings from* **A**, *Case 1,* **B**, *Case 2,* **C**, *Case 3, and* **D**, *Case 4.* **A-D**, *BRAF V600E is wildtype in all cases.* **A-C**, *Cases 1 to 3 have a TERT promotor C228T mutation.* **D**, *TERT promotor C228/C250 are wildtype in Case 4.* **A-C**, *Cases 1 and 3 show heterozygous deletion in CDKN2A/2B.* **B**, *CDKN2A/2B is normal in Case 2, and* **D**, *there is no amplification in Case 4 (ratio <2.0).*

CD34 is a neuronal precursor marker and may facilitate the differential diagnosis between PXA and diffusely infiltrating malignant tumors.[25] However, CD34 is known to be highly expressed in a subset of GBM as well.[26] In our cases, the histopathological and immunohistochemical findings were consistent with those of PXA.

The *BRAF* V600E mutation is observed in approximately 60% to 80% of all PXA cases.[3,27-30] The frequency of *BRAF* V600E mutation is slightly lower in patients with APXA (57%-75%) than in patients with grade II PXA (63%-79.2%).[5,7,28-30] Furthermore, it has been observed in 100% and 38% of pediatric and adult PXA patients, respectively.[28] PXA with the *BRAF* V600E mutant was reported a more favorable prognosis than PXA with the *BRAF* wildtype.[5,7,10] Approximately 2% of GBMs are known to harbor the *BRAF* V600E mutation as well.[28] None of our patients' tumors had the *BRAF* V600E mutation. In this study, we only performed direct sequencing around the V600E mutation hotspot. Although frame deletions within *BRAF* exon and less often *BRAF* fusions were described, there are very few studies which specifically address these and mutation other than *BRAF* V600E are considered very rare.[13,31]

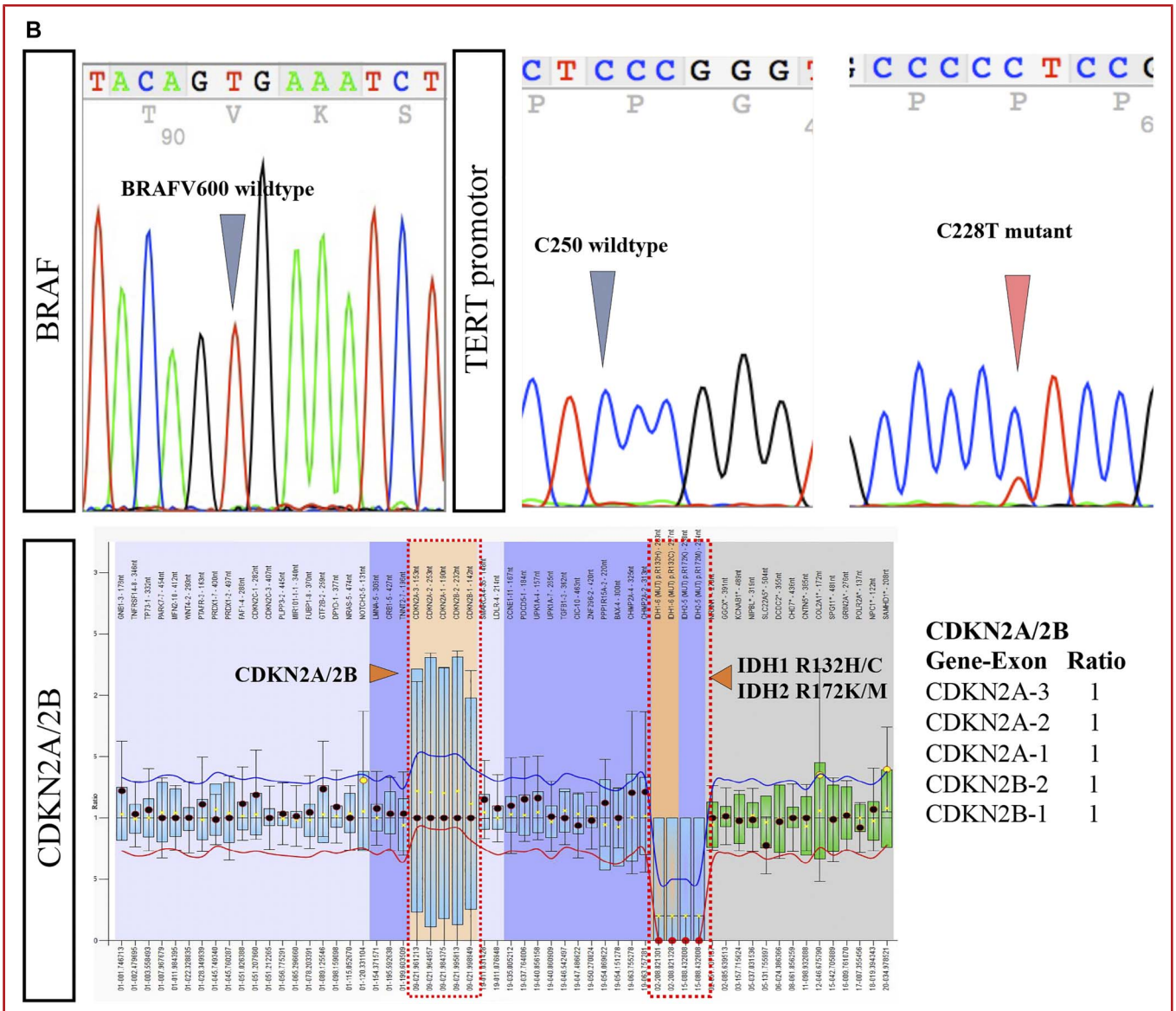

FIGURE 3. *Continued.*

Marucci et al[32] reported that MGMT promotor methylation was rare in PXA and that TMZ may be ineffective in treatment for aggressive PXA. MGMT might be a poor prognostic factor for both high-grade glioma and PXA.[14,32] Immunohistochemistry revealed MGMT expression in all 4 patients.

The frequency of homozygous deletion of chromosome 9 coding *CDKN2A/2B* is 60% to 87% in all PXA, 83% in grade II PXA, and 93% in APXA, respectively.[7,33] In our series, 2 patients with poor prognosis showed heterozygous deletions of *CDKN2A/2B* (Cases 1 and 3); however, another patient (Case 2) with wildtype *CDKN2A/2B* also died 9 months after treatment. *CDKN2A/2B* homozygous deletions have been reported to be as high as 86% in primary GBM.[34]

TERT promotor mutations are relatively rare in PXA (4% in grade II PXA and 23% in APXA).[35] However, a different paper reported 7 of 15 (47%) of *TERT* alterations in APXA, including 5 (71.4%) hotspot mutations. *TERT* promotor mutations might be associated with anaplastic progression.[27] Some secondary APXAs acquire *TERT* promotor mutations during recurrence.[27,36,37] A previous study reported a strong association between *TERT* promotor mutation and shorter survival; furthermore, no patients with *TERT* promotor mutations survived after 5 years.[10,29] As observed in our series, C228T mutation is more common in APXA and primary GBM[38]; contrastingly, C250T mutations are common in epithelioid glioblastoma.[36]

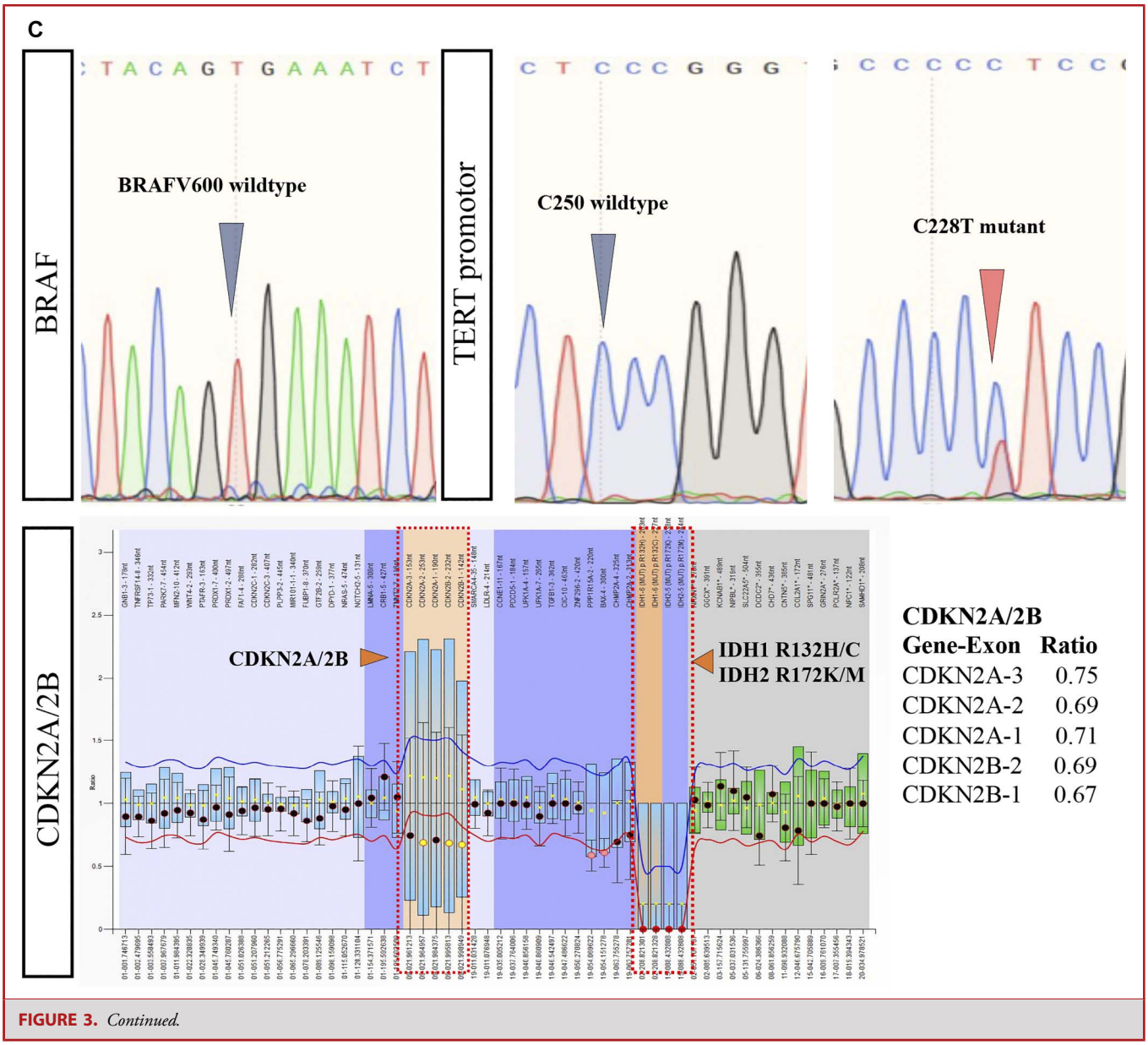

FIGURE 3. *Continued.*

In our series, the 3 patients with poorer prognosis showed bilateral FLAIR hyperintense lesions on MRI and had tumors with *TERT* promotor mutations. The typical MRI features of APXA include supratentorial and superficial location, obvious peritumoral edema, and heterogeneous and leptomeningeal Gd enhancement.[39] Multiple lesions, including multicentric or disseminated lesions in the cerebral hemispheres and/or spinal cord, are extremely rare at diagnosis of PXA and APXA.[40,41]

By contrast, a patient without *TERT* promotor mutation who presented unilateral FLAIR hyperintense and Gd-enhancing lesions has survived without recurrence for >2.5 years. That case had a unilateral Gd-enhancing lesion and surrounding FLAIR hyperintense lesion with *TERT* promotor wildtype. This is suggestive of relatively good survival and therapeutic response despite the high MIB1 LI (39.5%). In GBM, there are reports that MIB1 LI does not predict patient survival and response to additional therapies and does not significantly alter PFS and OS.[42,43]

Methylation classifier analysis revealed that these 4 cases were not classified as PXA. Capper et al[21] reported that 3 histological APXA cases were all classified as glioblastoma, IDH-wildtype, mesenchymal type. Furthermore, Ebrahimi et al[10] also reported that in 144 histological PXA, only 62 cases were judged as PXA by methylation classifier.

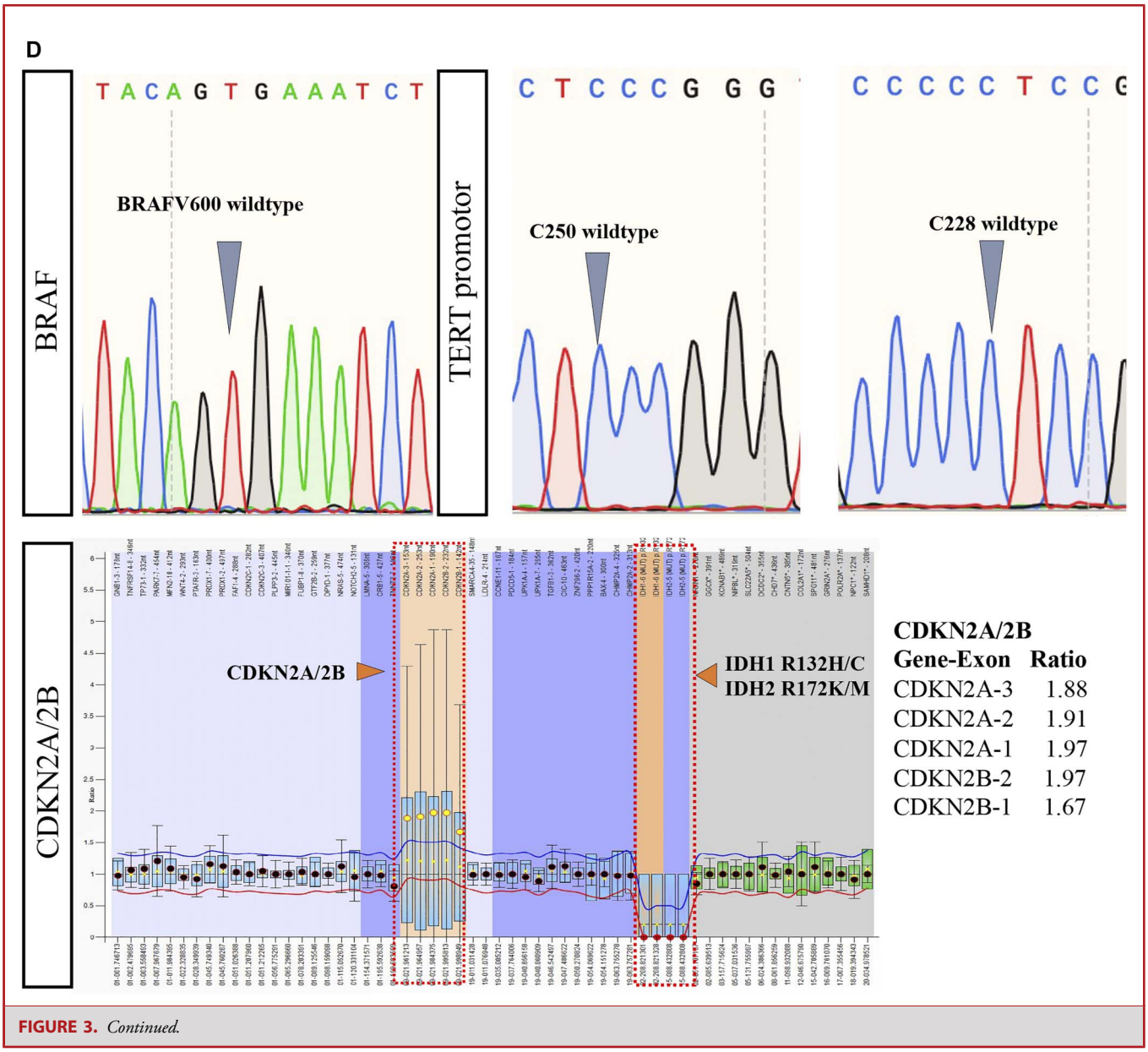

FIGURE 3. *Continued.*

In our cases, none of the cases diagnosed as APXA by histological features were classified as APXA by methylation classification. Importantly, APXA and GBM can be difficult to distinguish by histological or genetic analysis, and methylation classification should be performed, especially in cases showing diffuse infiltration on MRI.

Limitations

This report included only 4 patients from a single institution, and previous reports investigating the molecular features of histopathological APXA cases are mostly limited to small case series. Large-scale studies and thorough genetic analysis are warranted to clarify the prognosis and characteristic genetic profiles of histopathological APXA in middle-aged and older patients.

CONCLUSION

Methylation classifier should be performed to distinguish between APXA and GBM IDH-wildtype, especially in cases showing diffusely infiltrating lesions on MRI and harboring

TABLE 3. Results of Genetic Analysis and Methylation Classifier

Case	Age	M/F	BRAF V600E (sanger)	CDKN2A/B (MLPA)	*TERT*-p (sanger)	IDH1/2 (sanger)	p53 (IHC)	Methylation classifier (v12.5)		
								Methylation classes	Calibrated score	Interpretation
1	74	M	WT	Heterozygous deletion	C228T mutant	WT	+	Glioblastoma, IDH-wildtype, mesenchymal type	0.87849	No match
								MC glioblastoma, IDH-wildtype, mesenchymal subtype, subclass B (novel)	0.45519	No match
								MC glioblastoma, IDH-wildtype, mesenchymal subtype	0.42329	No match
2	84	M	WT	WT	C228T mutant	WT	+	MC glioblastoma, IDH-wildtype, mesenchymal subtype	0.99999	Match
3	52	F	WT	Heterozygous deletion	C228T mutant	WT	+	MC glioblastoma, IDH-wildtype, mesenchymal subtype	0.99998	Match
4	69	M	WT	WT	WT	WT	+	MC glioblastoma, IDH-wildtype, mesenchymal subtype, subclass B (novel)	0.98434	Match

IDH, isocitrate dehyodrogenase; IHC, immunohistochemistry; MC, methylation class; MLPA, multiplex ligation-dependent probe amplification; *TERT*-p, telomerase reversed transcriptase promotor; WT, wildtype.

TERT promoter mutations, as they can be difficult to differentiate histologically and genetically.

Funding

This study did not receive any funding or financial support.

Disclosures

The authors have no personal, financial, or institutional interest in any of the drugs, materials, or devices described in this article.

REFERENCES

1. Kepes JJ, Rubinstein LJ, Eng LF. Pleomorphic xanthoastrocytoma: a distinctive meningocerebral glioma of young subjects with relatively favorable prognosis. A study of 12 cases. *Cancer*. 1979;44(5):1839-1852.
2. Perkins SM, Mitra N, Fei W, Shinohara ET. Patterns of care and outcomes of patients with pleomorphic xanthoastrocytoma: a SEER analysis. *J Neurooncol*. 2012;110(1):99-104.
3. Dias-Santagata D, Lam Q, Vernovsky K, et al. BRAF V600E mutations are common in pleomorphic xanthoastrocytoma: diagnostic and therapeutic implications. *PLoS One*. 2011;6(3):e17948.
4. Mallick S, Benson R, Melgandi W, Giridhar P, Rath GK. Grade II pleomorphic xanthoastrocytoma; a meta-analysis of data from previously reported 167 cases. *J Clin Neurosci*. 2018;54:57-62.
5. Ida CM, Rodriguez FJ, Burger PC, et al. Pleomorphic Xanthoastrocytoma: natural history and long-term follow-up. *Brain Pathol*. 2015;25(5):575-586.
6. Tonse R, Gupta T, Epari S, et al. Impact of WHO 2016 update of brain tumor classification, molecular markers and clinical outcomes in pleomorphic xanthoastrocytoma. *J Neurooncol*. 2018;136(2):343-350.
7. Vaubel RA, Caron AA, Yamada S, et al. Recurrent copy number alterations in low-grade and anaplastic pleomorphic xanthoastrocytoma with and without BRAF V600E mutation. *Brain Pathol*. 2018;28(2):172-182.
8. Ono T, Sasajima T, Shimizu H, et al. Molecular features and prognostic factors of pleomorphic xanthoastrocytoma: a collaborative investigation of the Tohoku brain tumor study group. *Neurol Med Chir*. 2020;60(11):543-552.
9. Choudry UK, Khan SA, Qureshi A, Bari E. Primary anaplastic pleomorphic xanthoastrocytoma in adults. Case report and review of literature. *Int J Surg Case Rep*. 2016;27:183-188.
10. Ebrahimi A, Korshunov A, Reifenberger G, et al. Pleomorphic xanthoastrocytoma is a heterogeneous entity with pTERT mutations prognosticating shorter survival. *Acta Neuropathol Commun*. 2022;10(1):5.
11. Lin Z, Yang R, Zheng H, et al. Pleomorphic xanthoastrocytoma, anaplastic pleomorphic xanthoastrocytoma, and epithelioid glioblastoma: case series with clinical characteristics, molecular features and progression relationship. *Clin Neurol Neurosurg*. 2022;221:107379.
12. Mahajan S, Dandapath I, Garg A, Sharma MC, Suri V, Sarkar C. The evolution of pleomorphic xanthoastrocytoma: from genesis to molecular alterations and mimics. *Lab Invest*. 2022;102(7):670-681.
13. Shaikh N, Brahmbhatt N, Kruser TJ, et al. Pleomorphic xanthoastrocytoma: a brief review. *CNS Oncol*. 2019;8(3):cns39.
14. Ogura R, Tsukamoto Y, Natsumeda M, et al. Immunohistochemical profiles of IDH1, MGMT and P53: practical significance for prognostication of patients with diffuse gliomas. *Neuropathology*. 2015;35(4):324-335.
15. Tanaka G, Nakazato Y. Automatic quantification of the MIB-1 immunoreactivity in brain tumors. *Int Congress Ser*. 2004;1259:15-19.
16. Nobusawa S, Lachuer J, Wierinckx A, et al. Intratumoral patterns of genomic imbalance in glioblastomas. *Brain Pathol*. 2010;20(5):936-944.
17. Kanemaru Y, Natsumeda M, Okada M, et al. Dramatic response of BRAF V600E-mutant epithelioid glioblastoma to combination therapy with BRAF and MEK inhibitor: establishment and xenograft of a cell line to predict clinical efficacy. *Acta Neuropathol Commun*. 2019;7(1):119.
18. Nakajima N, Nobusawa S, Nakata S, et al. BRAF V600E, TERT promoter mutations and CDKN2A/B homozygous deletions are frequent in epithelioid glioblastomas: a histological and molecular analysis focusing on intratumoral heterogeneity. *Brain Pathol*. 2018;28(5):663-673.
19. Jeuken J, Cornelissen S, Boots-Sprenger S, Gijsen S, Wesseling P. Multiplex ligation-dependent probe amplification: a diagnostic tool for simultaneous identification of different genetic markers in glial tumors. *J Mol Diagn*. 2006;8(4):433-443.

20. Jeuken J, Sijben A, Alenda C, et al. Robust detection of EGFR copy number changes and EGFR variant III: technical aspects and relevance for glioma diagnostics. *Brain Pathol*. 2009;19(4):661-671.
21. Capper D, Jones DTW, Sill M, et al. DNA methylation-based classification of central nervous system tumours. *Nature*. 2018;555(7697):469-474.
22. Rutkowski MJ, Oh T, Niflioglu GG, Safaee M, Tihan T, Parsa AT. Pleomorphic xanthoastrocytoma with anaplastic features: retrospective case series. *World Neurosurg*. 2016;95:368-374.
23. Hirose T, Ishizawa K, Sugiyama K, Kageji T, Ueki K, Kannuki S. Pleomorphic xanthoastrocytoma: a comparative pathological study between conventional and anaplastic types. *Histopathology*. 2007;52(2):183-193.
24. Schmidt Y, Kleinschmidt-DeMasters BK, Aisner DL, Lillehei KO, Damek D. Anaplastic PXA in adults: case series with clinicopathologic and molecular features. *J Neurooncol*. 2013;111(1):59-69.
25. Reifenberger G, Kaulich K, Wiestler OD, Blümcke I. Expression of the CD34 antigen in pleomorphic xanthoastrocytomas. *Acta Neuropathol*. 2003;105(4):358-364.
26. Michaelsen SR, Urup T, Olsen LR, Broholm H, Lassen U, Poulsen HS. Molecular profiling of short-term and long-term surviving patients identifies CD34 mRNA level as prognostic for glioblastoma survival. *J Neurooncol*. 2018;137(3):533-542.
27. Phillips JJ, Gong H, Chen K, et al. The genetic landscape of anaplastic pleomorphic xanthoastrocytoma. *Brain Pathol*. 2019;29(1):85-96.
28. Schindler G, Capper D, Meyer J, et al. Analysis of BRAF V600E mutation in 1,320 nervous system tumors reveals high mutation frequencies in pleomorphic xanthoastrocytoma, ganglioglioma and extra-cerebellar pilocytic astrocytoma. *Acta Neuropathol*. 2011;121(3):397-405.
29. Vaubel R, Zschernack V, Tran QT, et al. Biology and grading of pleomorphic xanthoastrocytoma-what have we learned about it? *Brain Pathol*. 2021;31(1):20-32.
30. Koelsche C, Sahm F, Wohrer A, et al. BRAF-mutated pleomorphic xanthoastrocytoma is associated with temporal location, reticulin fiber deposition and CD34 expression. *Brain Pathol*. 2014;24(3):221-229.
31. Horbinski C. To BRAF or not to BRAF: is that even a question anymore? *J Neuropathol Exp Neurol*. 2013;72(1):2-7.
32. Marucci G, Morandi L. Assessment of MGMT promoter methylation status in pleomorphic xanthoastrocytoma. *J Neurooncol*. 2011;105(2):397-400.
33. Weber RG, Hoischen A, Ehrler M, et al. Frequent loss of chromosome 9, homozygous CDKN2A/p14(ARF)/CDKN2B deletion and low TSC1 mRNA expression in pleomorphic xanthoastrocytomas. *Oncogene*. 2007;26(7):1088-1097.
34. Neilsen BK, Sleightholm R, McComb R, et al. Comprehensive genetic alteration profiling in primary and recurrent glioblastoma. *J Neurooncol*. 2019;142(1):111-118.
35. Koelsche C, Sahm F, Capper D, et al. Distribution of TERT promoter mutations in pediatric and adult tumors of the nervous system. *Acta Neuropathol*. 2013;126(6):907-915.
36. Furuta T, Miyoshi H, Komaki S, et al. Clinicopathological and genetic association between epithelioid glioblastoma and pleomorphic xanthoastrocytoma. *Neuropathology*. 2018;38(3):218-227.
37. Hosono J, Nitta M, Masui K, et al. Role of a promoter mutation in TERT in malignant transformation of pleomorphic xanthoastrocytoma. *World Neurosurg*. 2019;126:624-630.
38. Arita H, Yamasaki K, Matsushita Y, et al. A combination of TERT promoter mutation and MGMT methylation status predicts clinically relevant subgroups of newly diagnosed glioblastomas. *Acta Neuropathol Commun*. 2016;4(1):79.
39. She D, Liu J, Xing Z, Zhang Y, Cao D, Zhang Z. MR imaging features of anaplastic pleomorphic xanthoastrocytoma mimicking high-grade astrocytoma. *AJNR Am J Neuroradiol*. 2018;39(8):1446-1452.
40. Montano N, Papacci F, Cioni B, et al. Primary multicentric pleomorphic xanthoastrocytoma with atypical features. *J Clin Neurosci*. 2013;20(11):1605-1608.
41. Yan J, Cheng J, Liu F, Liu X. Pleomorphic xanthoastrocytomas of adults: MRI features, molecular markers, and clinical outcomes. *Sci Rep*. 2018;8(1):14275.
42. Detti B, Scoccianti S, Maragna V, et al. Pleomorphic xanthoastrocytoma: a single institution retrospective analysis and a review of the literature. *Radiol Med*. 2022;127(10):1134-1141.
43. Moskowitz SI, Jin T, Prayson RA. Role of MIB1 in predicting survival in patients with glioblastomas. *J Neurooncol*. 2006;76(2):193-200.

Acknowledgments

The authors acknowledge C. Tanda, J. Takasaki, Y. Tanaka, A. Nakahara, S. Nigorikawa, A. Yoshii, and T. Eda for advice and their technical assistance and T. Uzuka, T. Kobayashi, M. Isogawa, H. Takahashi, and H. Aoki for clinical management and guidance.

Supplemental digital content *is available for this article at neurosurgerypractice-online.com.*

Supplemental Digital Content 1. Table. List of forward and reverse primers used in sanger sequence.

Supplemental Digital Content 2. Table. List of antibodies used in immunohistochemical staining.

Supplemental Digital Content 3. Figure. Head MRI findings and head CT images of irradiation planning of case 1 (A, B) and case 2 (C, D). The right panel shows the axial gadolinium-enhanced T1WI, and the left panel shows the axial FLAIR image. Upper panels show preoperation images, middle panels show postoperation images, and lower at the time of recurrence (A). Despite left tumor resection and bilateral local irradiation (60 Gy/30 fr) with TMZ, bilateral tumors showed progression 4 month after, and stereotactic radiotherapy (40 Gy/8 fr) was performed. Planning CT scan images depicting the primary irradiation field are shown in the upper panel and secondary irradiation area in lower panel (B). The right panel shows the axial gadolinium-enhanced T1WI, and the left panel shows the axial FLAIR image. Upper panels show preoperation images, middle panels show postoperation images, and lower panels at the time of recurrence (C). Planning CT scan images showing the primary irradiation area (D). In case 2, the tumor in irradiation field showed progression. This case was transferred to best supportive case without secondary radiotherapy.

Supplemental Digital Content 4. Figure. Head MRI findings and head CT images of irradiation planning of case 3(A, B) and case 4 (C, D). The right panel shows the axial gadolinium-enhanced T1WI, and the left panel shows the axial FLAIR image. Upper panels show preoperation images, middle panels show postoperation images, and lower at the time of recurrence (A). Bilateral thalamic FLAIR hyperintense lesion showed regression by local irradiation (60 Gy/30 fr) with TMZ. However, relapse was observed in the bilateral cerebellar hemispheres at 15 posttreatment months, accompanied with ataxia. Subsequently, stereotactic radiotherapy of the new lesions was performed. Planning CT scan images of the primary irradiation area are shown in the upper panel and secondary irradiation area in the lower panel (B). The right panel shows the axial gadolinium-enhanced T1WI, and the left panel shows the axial FLAIR image. Upper panels show preoperation images, and lower panels show postoperation images (C). Primary irradiation area shown as planning CT scan images (D). In case 4, the patient survived for >2.5 years without recurrence after surgery.

Supplemental Digital Content 5. Figure. Kaplan-Meier curve of PFS and overall survival of the 4 cases. The 1-year and 2-year survival rates were 50% and 25%, respectively. The mean postrecurrence survival period of 3 patients was 4.3 month (range: 3-5 months).